Technical University of Denmark

DTU

Electrochemical studies of the molten system K2NbF7-Na2O-Nb-(LiF-NaF-KF)(eut) at 700 degrees C

Rosenkilde, C.; Vik, A.; Østvold, T.; Christensen, Erik; Bjerrum, Niels J.

Link back to DTU Orbit

DTU Library
Technical Information Center of Denmark

Electrochemical Studies of the Molten System K₂NbF₇-Na₂O-Nb-(LiF-NaF-KF)eut at 700°C

Christian Rosenkilde,[a],* Aasmund Vik,[b] Terje Østvold,[b] Erik Christensen,[c] and Niels J. Bjerrum[c],*

[a]*Norsk Hydro Research Center, N3901 Porsgrunn, Norway*
[b]*Department of Chemistry, Norwegian University of Science and Technology, 7491 Trondheim, Norway*
[c]*Department of Chemistry, Technical University of Denmark, DK-2800 Lyngby, Denmark*

Various voltammetric methods have been used to study FLINAK (LiF-NaF-KF eutectic melt 46.5-11.5-42 mol %) melts containing about 1 mol % niobium-fluoro and -oxofluoro complexes with Nb in oxidation states (V) and (IV) at 700°C and varying amounts of Na₂O in the range $0 < n_O^o/n_{Nb}^o < 7$. A slow, spontaneous reduction of Nb(V)-fluoro complexes to Nb(IV)-fluoro complexes was observed in the absence of Nb metal. With a stoichiometric amount of Nb metal, Nb(V) is reduced rapidly to Nb(IV) according to the reaction $4NbF_7^{2-} + Nb \rightleftharpoons 5NbF_x^{(x-4)-}$. The solubilities of Nb₂O₅ and KNbO₃ in FLINAK were measured and found to be 1.8 and 0.13 mol %, respectively. The following reactions probably occur when increasing amounts of oxide are added to a melt originally containing $NbF_x^{(x-4)-}$: $NbF_x^{(x-4)-} + O^{2-} \rightleftharpoons$ Nb(IV)-mono-oxo-fluoride + fluoride, 5Nb(IV)-mono-oxo-fluoride + $O^{2-} \rightleftharpoons 4NbO_2F_4^{3-} + Nb$, and $NbO_2F_4^{3-} + O^{2-} + Alk^+ \rightleftharpoons AlkNbO_3(s) + 4F^-$ ($Alk^+ = Li^+$, Na^+, or K^+). At oxide to niobium molar ratios higher than three, AlkNbO₃(s) redissolves, and at $n_O^o/n_{Nb}^o > 4$, all Nb and O added are dissolved. Strong indications of the coexistence of the oxygen rich Nb(V)OF complexes and O^{2-} ions in FLINAK at $n_O^o/n_{Nb}^o > 4$ have been found. An equilibrium/sampling/analysis technique was also used to study this system without Nb metal added. The results mainly agree with the results of the voltammetric studies. However, no indications of spontaneous reduction of Nb(V) to Nb(IV) were observed, even after 24 h. © 2000 The Electrochemical Society. S0013-4651(99)12-112-8. All rights reserved.

The chemical and electrochemical properties of niobium and tantalum in alkali-fluoride melts[1-10] and chloride melts[10-16] have been studied extensively during the last decade. The motivation for this work is mainly twofold. First, the very high stability of niobium and tantalum against aqueous acids makes steel parts electroplated with these metals highly corrosion resistant and, consequently, useful for many purposes. Second, these systems are interesting from a scientific point of view due to the strong complex-forming ability of niobium and tantalum ions. Moreover, in these complexes, Nb and Ta may exist in various oxidation states. This, together with the complex-forming ability, leads to rather complicated chemical systems. In spite of a lot of previous work, both the chemistry and electrochemistry in fluoride and chloride melts containing oxides are still matters of discussion. Further investigations are therefore justified.

In the present study we have focused on the electrochemistry and bulk properties of niobium ions in FLINAK (LiF-NaF-KF eutectic melt 46.5-11.5-42 mol %) at 700°C. In particular, we have studied melts where niobium ions are in equilibrium with Nb metal and controlled amounts of oxide in the melt. This is interesting since niobium metal is present during electroreduction of Nb. Equilibrium between Nb ions in the melt and Nb metal will therefore be established.

Von Barner *et al.*[1] investigated Nb(V)-fluorides and -oxofluorides in FLINAK by Raman spectroscopy, and the complexes NbF_7^{2-}, $NbOF_5^{2-}$, and $NbO_2F_4^{3-}$ were suggested to be stable in the melt. Indications of complexes even richer in oxygen were also given. Von Barner *et al.*[1] did not determine, however, the oxide and niobium concentrations in the melt analytically. Due to the precipitation of AlkNbO₃(s) (Alk = Li^+, Na^+, or K^+) at molar ratios of oxide to niobium $2 < n_O^o/n_{Nb}^o < 3$ and dissolution at $n_O^o/n_{Nb}^o > 3$ observed by Matthiesen *et al.*[17] inaccurate molar ratios of oxide to niobium were probably given by von Barner *et al.*[1] Matthiesen *et al.*[17] studied Nb(IV) in FLINAK at various Na₂O concentrations up to $n_O^o/n_{Nb}^o \approx 10$. The Nb(IV) was prepared by *in situ* reduction of K₂NbF₇ with the stoichiometric amount of Nb metal. They found that the amounts of added and analyzed oxide in the melt were identical up to the molar ratio $n_O^o/n_{Nb}^o = 1$. Above this ratio, the Nb concentration in the melt decreased up to $n_O^o/n_{Nb}^o \approx 2.2$. Together with an observed slope lower than one of oxide analyzed *vs.* oxide added, the results indicated precipitation of a Nb(IV) oxide compound. The reaction $3NbOF_5^{3-} + 2 O^{2-} \rightleftharpoons NbOF_2(s) + 2NbO_2F_4^{4-} + 5F^-$ was

suggested to explain the results. In the composition region $2.2 < n_O^o/n_{Nb}^o < 3$, Nb(IV) decreased even faster, and decreasing O^{2-} concentrations were measured, indicating that a compound of the type $Alk_2NbO_3(s)$ was precipitating. At $3 < n_O^o/n_{Nb}^o < 4$, the solid precipitate dissolved, and, according to stoichiometry, the dominant reaction was $Alk_2NbO_3(s) + xF^- + O^{2-} \rightleftharpoons NbO_4F_x^{(4+x)-} + 2Alk^+$. Recently Vik *et al.*[18] showed by Raman spectroscopy that a melt consisting of K₂NbF₇ in FLINAK with varying Na₂O concentrations up to $n_O^o/n_{Nb}^o = 8$ probably contained several Nb(V)-O-F complexes with varying stoichiometry depending on the O/Nb molar ratio. For $n_O^o/n_{Nb}^o < 1$, the monomeric $NbOF_5^{2-}$ ion was present. For $1 < n_O^o/n_{Nb}^o < 2$ both $NbOF_5^{2-}$ and $NbO_2F_4^{3-}$ occurred. At higher ratios it is possible that $NbO_3F_3^{4-}$, $NbO_4F_2^{5-}$, and corner shared NbO₆ octahedra linked together in a network are present in the melt.[1,18-21]

Electrochemical work[2] has shown that good Nb deposits were obtained from melts equilibrated with Nb metal and with small and controlled amounts of oxide present. It was further found that small amounts of oxide in the melt increased the current efficiency for the deposition process. In the present work the effect of larger amounts of oxide compared to the amount of Nb ions in the melt is studied. Since there has been some debate as to the stability of Nb-oxofluoride ions with niobium in oxidation states different from five, this matter has also been studied more closely. Previous voltammetric investigations in alkali fluoride[2,4,22] or alkali-fluoride-chloride melts[5,23] have not shown a reduction step belonging to the reduction of $NbOF_5^{2-}$ to a soluble product, *e.g.*, a Nb(IV)-oxofluoride complex. On the other hand, adding Nb metal to a melt containing $NbOF_5^{2-}$, Christensen *et al.*[2] observed dissolution of Nb metal, indicating reduction of Nb(V) in $NbOF_5^{2-}$ to a Nb(IV) species.

The reader will find some discrepancies in the results obtained with the different methods used in the present work. We have not been able to resolve these, but hope that the work presented will help the scientific community to resolve the discrepancies.

Experimental

Two experimental techniques have been used. The first method was based on equilibration, sampling, and analysis of the melt. The analysis of the samples was performed with inductively coupled plasma (ICP) for Nb and the carbothermal-reduction technique using LECO TC-436 for oxide in the melt.[17] The experimental procedure has been published elsewhere.[17] The electrochemical techniques involved cyclic voltammetry, linear sweep voltammetry, staircase

* Electrochemical Society Active Member.

voltammetry, and square wave voltammetry. These methods are available through the use of a computer-controlled potentiostat/galvanostat model M273, Princeton Applied Research. All voltammograms were recorded with more than 85% of full ohmic (IR) compensation. The IR drop was measured with a Solartron 1255 HF frequency response analyzer connected to the PAR M273 potentiostat. The electrochemical cell was a glassy carbon crucible (Carbon-Lorraine V25, diam 50 mm) with a common three-electrode system. Platinum has proved to be inert in the melts, and therefore Pt quasi-reference (wire diam 0.5 mm), counter (sheet, area 2 cm^2), and working (wire diam 0.5 mm) electrodes were employed. Working electrodes made of glassy carbon (SU2000, diam 1 mm) were also used to study oxidation of oxide-containing species. The electrodes were connected to stainless steel rods. The area of the working electrodes was determined by immersing the electrode at several depths and measuring a suitable voltammetric peak current at each depth. The immersion depth was controlled by a scaled micrometer screw. In this way a linear relationship between current and immersion depth was obtained. The current is proportional to the surface area of the electrode since the current density is the same. The relationship between the surface area and the immersion depth is thus given by $A = A_0 + \pi dh$, where A_0 is the area when the electrode just dips into the electrolyte (at zero immersion), d is the electrode diameter, and h the immersion depth. A_0 is determined from the intercept of the line in a plot of area *vs.* immersion depth. A_0 is the sum of the area of the bottom of the electrode and the surface covered by the meniscus. The furnace used in the experiments was a water-cooled three-zone Kanthal wound vertical tubular furnace with a nickel inner tube. The temperature was measured with a type-K thermocouple positioned just outside the crucible. Figure 1 shows a drawing of the cell.

A Pt quasi reference is usually inferior to a proper reference electrode. In the highly corrosive niobium-containing fluoride melts, however, design of a true reference electrode that does not contaminate the melt has proved to be very difficult. Furthermore, in the presence of Nb(V), Nb(IV) ions, or Nb metal in the melt and at constant melt composition, the potential of the Pt quasi-reference electrode has proved to be stable for times long enough to allow recording of voltammograms with low sweep rates, *i.e.,* several minutes. The Pt quasi-reference electrode was therefore found to be suitable for the present work, where the amount of impurities was to be kept at a minimum.

The observed spontaneous reduction of Nb(V)-fluorides to Nb(IV)-fluoride in the melt introduces some experimental problems. In the experiments where the Nb(V)-fluorides were studied electrochemically the experiments were performed as fast as possible to avoid significant amounts of Nb(IV) to formation. In experiments where Nb(V) is to be reduced with Nb metal, the amount of Nb(V) in the melt shortly before addition of Nb metal must be known to calculate the amount of Nb metal dissolved according to Eq. 4. This is important since it is necessary to know the total amount of Nb ions in solution before starting additions of Na$_2$O. According to Eq. 4, the amount of Nb metal dissolved would be 1/4 the amount of Nb(V) added when there is no spontaneous reduction, but with spontaneous reduction less Nb metal is dissolved. Since the reduction of Nb(V) to Nb(IV) is much faster in the presence of Nb metal, one can, by knowing the amount of Nb(V) spontaneously reduced, calculate the precise amount of Nb metal dissolved. Since it is possible to monitor the degree of spontaneous reduction by voltammetry (cf. Fig. 6), the amount of Nb(V) reduced to Nb(IV) can be found. When necessary, this was done in the present voltammetric study.

All handling and weighing of the salts was performed in a dry box to avoid water contamination of the hygroscopic fluoride salts. The FLINAK mixture was prepared from recrystallized alkali fluorides (Merck, p.a.). K$_2$NbF$_7$ (>97% by analysis) was prepared according to Christensen *et al.,*[2] and Na$_2$O (>98% by acid titration) prepared from Na$_2$O$_2$ according to Horsby.[24] Nb was used as purchased (Goodfellow, >99%), as was Nb$_2$O$_5$ (CERAC, >99.95) and KNbO$_3$ (Hereaus, >99.8). The two latter salts were dried at 150°C before use. In the voltammetric studies, a crucible with 60 g of the

alkali fluoride weighed out according to the composition of FLINAK (LiF-NaF-KF: 46.5-11.5-42 mol %) was removed from the dry box and placed in the furnace, which was then evacuated. The furnace was left under vacuum at 350°C overnight. It was then filled with argon, and the temperature was raised to 700°C. An overpressure of 0.1 bar was maintained in the furnace by electronically controlled valves. Thus, the atmosphere in the furnace was practically the same during the whole experiment. The other salts were weighed in the dry box and removed from the box in an airtight container that was connected to the salt-addition tube. The salt-addition tube was built in such a way that neither the salt to be added nor the atmosphere in the furnace was in contact with air during addition.

The solubility studies using the equilibrium/sampling technique were performed in the same type of cell as described previously, but the furnace containing the cell was connected directly to a dry box. In this way all handling of salts was under the dry-box atmosphere.[17]
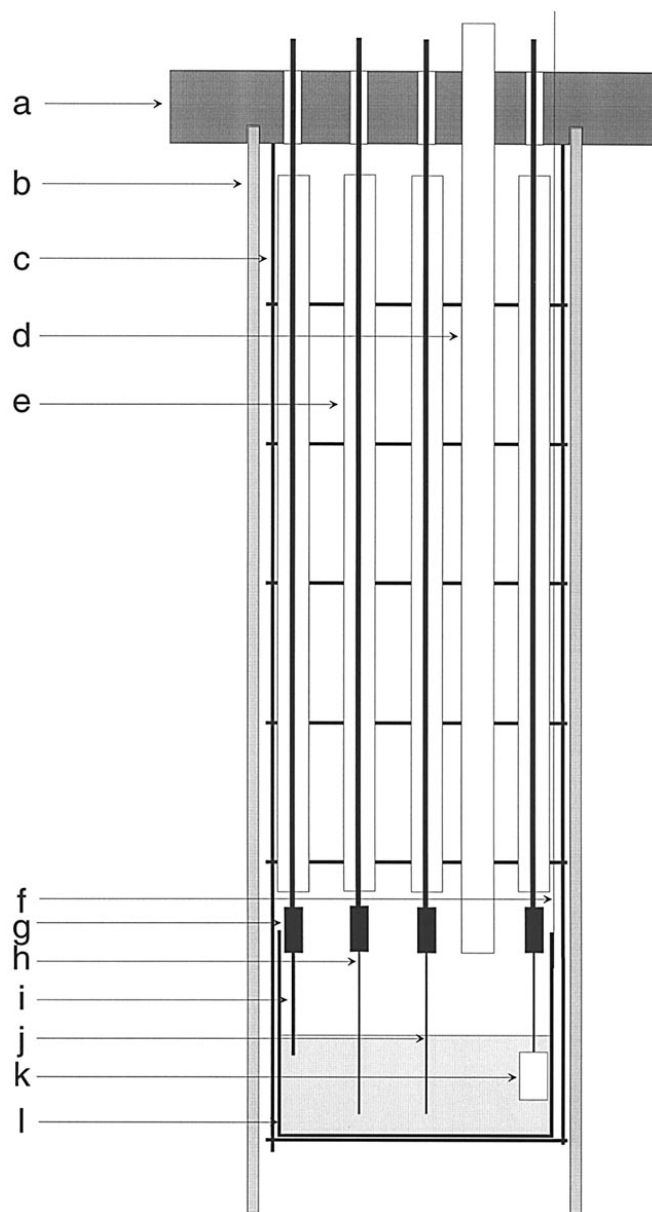
Figure 1. Drawing of the experimental cell: (a) brass cover, (b) furnace inner nickel tube, (c) stainless steel rods connected to the lid, (d) stainless steel addition tube, (e) alumina insulation tubes, (f) thermocouple, (g) stainless steel connection piece, (h) platinum quasi reference electrode, (i) glassy carbon working electrode, (j) platinum working electrode, (k) platinum counter electrode, (l) glassy carbon crucible.

The solubility studies were done at NTNU in Norway, while the electrochemical work was done at DTU in Denmark.

Results

Voltammograms of oxide-free melts.—Figure 2 shows a voltammogram of a FLINAK melt containing 0.8 mol % K_2NbF_7. The voltammogram has two reduction steps, R_1 and R_2, and two corresponding oxidation steps, Ox_1 and Ox_2. Voltammograms were recorded using sweep rates from 0.1 to 20 V s^{-1}, and a linear relationship between the peak currents of R_1 and R_2 and the square root of the sweep rate was observed. Included in Fig. 2 is a simulated voltammogram based on the following reduction mechanism assuming reversible and diffusion-controlled conditions
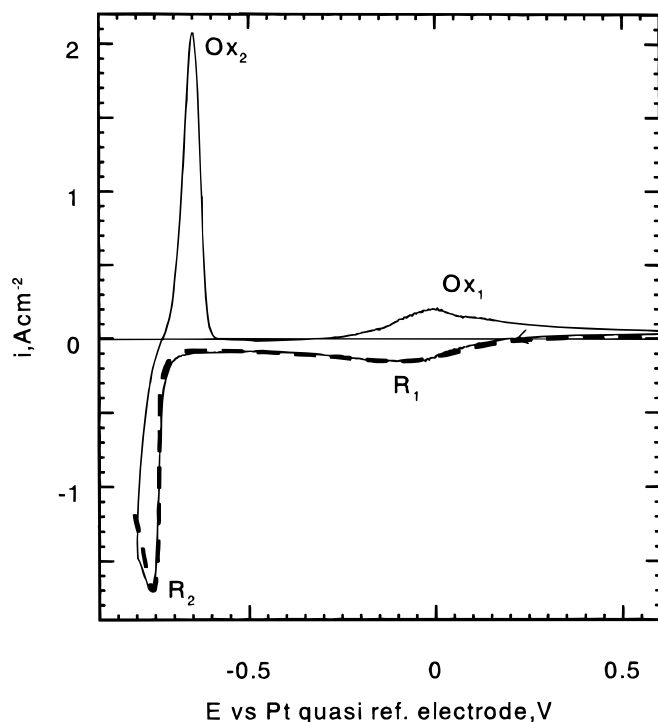
$$Nb^{5+} + e \rightleftharpoons Nb^{4+} \qquad [1]$$

and

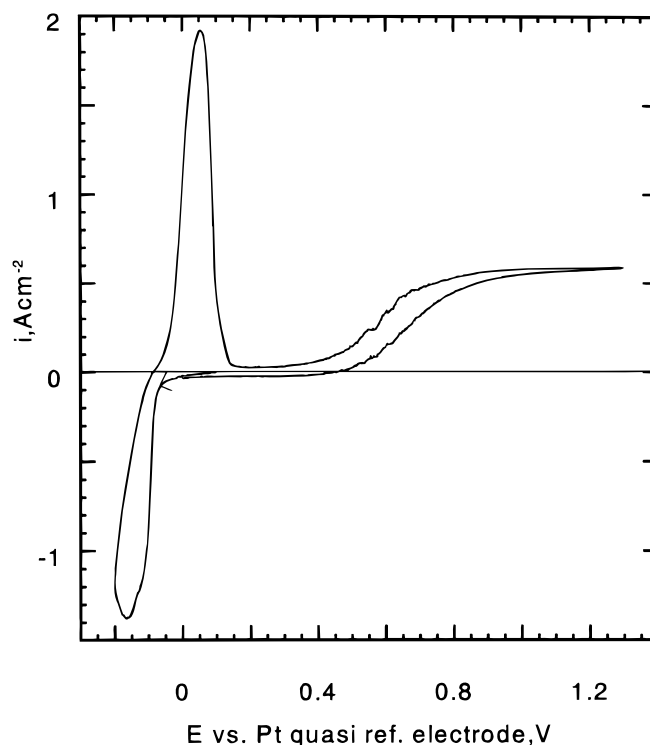$$Nb^{4+} + 4e^- \rightleftharpoons Nb \qquad [2]$$

The good agreement between the measured and simulated voltammogram together with the linear dependence of the peak current on the square root of the sweep rate show that the reductions given by Eq. 1 and 2 are reversible and diffusion controlled. This mechanism is in agreement with previous work in alkali-fluoride melts[2,4,18] and mixed alkali-chloride-fluoride melts.[21,22,26-28] Details concerning the simulation are previously described.[7] The diffusion coefficient of NbF_7^{2-} can be calculated using Eq. 3[29]

$$i_p = 0.4463nF\sqrt{\frac{nFDv}{RT}}c \qquad [3]$$

where n is the number of electrons transferred (in this case one), F is Faraday's number, D the diffusion coefficient, R the gas constant, T absolute temperature, v the sweep rate, and c the bulk concentration of the species undergoing reduction or oxidation. Using Eq. 3 with
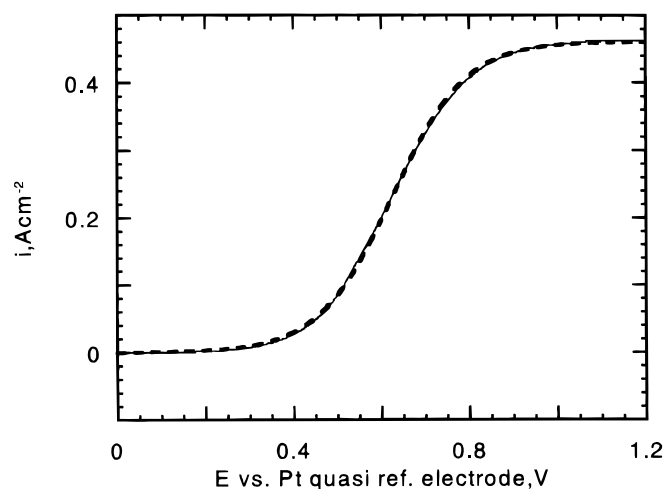

Figure 3. Cyclic voltammogram of a FLINAK melt containing 1 mol % K_2NbF_7 saturated with Nb metal at 700°C. Sweep rate 0.2 V s^{-1}. Pt reference, working, and counter electrodes. Area of working electrode 0.044 cm^2.

the measured voltammograms, a diffusion coefficient of NbF_7^{2-} in FLINAK at 700°C equal to 1.4×10^{-5} cm^2 s^{-1} is obtained.

Figure 3 shows a voltammogram of a FLINAK melt containing 1 mol % K_2NbF_7 saturated with Nb metal. The same reductions as those in Fig. 2 are observed, but there is a general anodic shift of the current. The reason for this is that the Nb(V) added as K_2NbF_7 is reduced by Nb metal. The oxidation state of Nb ions in equilibrium with Nb metal can be found from the voltammogram scanned at 5 mV s^{-1} in the positive direction from the rest potential in Fig. 4. The voltammogram is of the same melt as the voltammogram in Fig. 3.

Figure 2. Cyclic voltammogram of a FLINAK melt containing 0.81 mol % K_2NbF_7 at 700°C. Sweep rate: 0.2 V s^{-1}. Pt reference, working, and counter electrodes. Area of working electrode 0.044 cm^2. Included in the figure is a simulated LSV based on the reversible and diffusion-controlled reduction steps $Nb^{5+} + e^- \rightleftharpoons Nb^{4+}$ and $Nb^{4+} + 4e \rightleftharpoons Nb$. (—) Measured and (---) simulated.

Figure 4. LSV of a FLINAK melt containing 1 mol % K_2NbF_7 saturated with Nb metal at 700°C. Sweep rate 0.005 V s^{-1}. Pt reference, working, and counter electrodes. Area of working electrode 0.044 cm^2. Included in the figure is a curve based on the equation $E = E^0 + RT/F \ln(i/i_{lim} - 1)$ where all the symbols have their usual meaning. The curve was fitted using $E° = 0.625$ V and $i_{lim} = 0.461$ A cm^{-2}. (—) Measured and (---) simulated.

Voltammograms recorded at such low scan rates are usually very close to the steady-state situation where one can assume linear diffusion gradients within the Nernst layer. Under such conditions, limiting current values can be measured at sufficiently high overpotentials. One oxidation step is observed in Fig. 4, and a simulated curve based on an oxidation reaction involving transfer of one electron is included in the figure. Since the measured and simulated curves compare well, it is reasonable to conclude that Nb(IV)-fluoro complexes are the main species in the FLINAK melt at 700°C after reduction of Nb(V) with Nb metal. The reduction of Nb(V) by Nb metal therefore follows the reaction

$$4Nb^{5+} + Nb \rightleftharpoons 5Nb^{4+} \qquad [4]$$

Spontaneous reduction of Nb(V).—Figure 5 shows a voltammogram recorded at 5 mV s^{-1} of a FLINAK melt to which 1 mol % K_2NbF_7 was added. The voltammogram was recorded 23.75 h after addition of K_2NbF_7. The voltammogram shows two limiting current levels, one anodic at positive potentials and one cathodic at negative potentials. The anodic and cathodic limiting currents are plotted as functions of the time after addition of K_2NbF_7 in Fig. 6. Since the limiting current is directly proportional to the bulk concentration of the species undergoing reduction or oxidation, Fig. 6 shows that there is a spontaneous reduction of Nb(V) to Nb(IV) without addition of Nb metal. The cathodic limiting current represents the reduction of Nb(V) to Nb(IV), and the anodic limiting current the oxidation of Nb(IV) to Nb(V). Shortly after addition of K_2NbF_7, only a very low limiting current of the oxidation of Nb(IV) to Nb(V) is observed compared to the limiting current of the reduction of Nb(V) to Nb(IV). Consequently, there is practically no Nb(IV) in the melt compared to the amount of Nb(V). As the time after addition increases, however, the limiting current of the oxidation of Nb(IV) increases while the limiting current of the reduction of Nb(V) is decreasing. After about 100 h, almost all of the Nb(V) initially added is reduced to Nb(IV). Included in Fig. 6 are two fitted curves based on first-order reaction-rate expressions

$$\frac{di_{lim}}{dt} = \frac{FD_{Nb(V)}}{\delta}\frac{dc_{Nb(V)}}{dt} = -\frac{FD_{Nb(V)}}{\delta}kc_{Nb(V)} \qquad [5]$$

where t is time, D is the diffusion coefficient of Nb(V), δ is the thickness of the Nernst diffusion layer, k is the rate constant, and $c_{Nb(V)}$ the bulk concentration of Nb(V). For Nb(IV) the first-order rate expression becomes
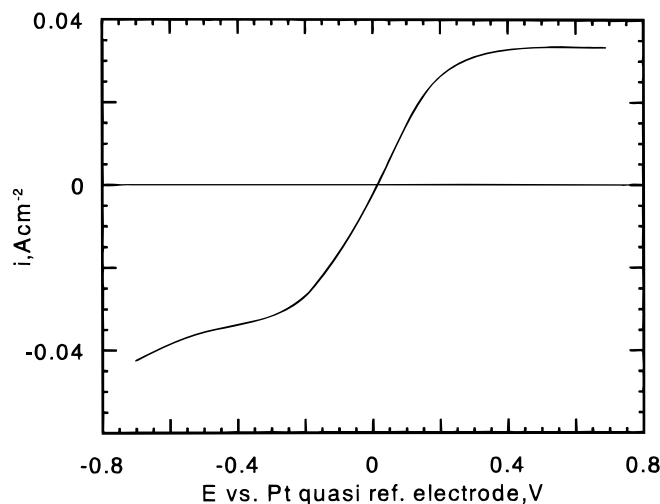
$$\frac{di_{lim}}{dt} = \frac{FD_{Nb(IV)}}{\delta}\frac{dc_{Nb(IV)}}{dt} = \frac{FD_{Nb(IV)}}{\delta}kc_{Nb(V)}$$

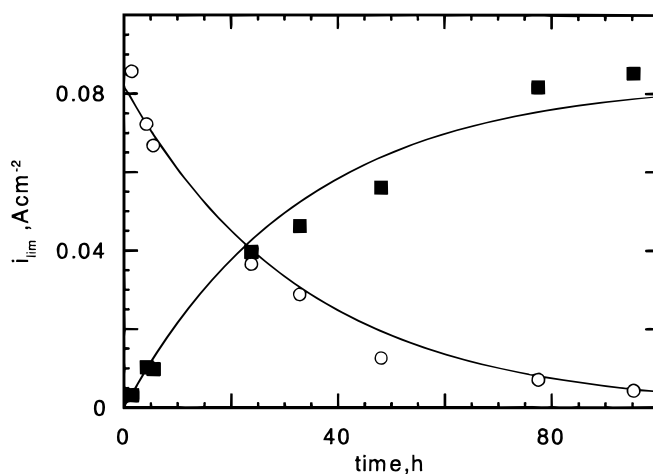$$= \frac{FD_{Nb(IV)}}{\delta}k(c_{Nb(V)}^0 - c_{Nb(IV)}) \qquad [6]$$

where $c_{Nb(V)}^0$ is the initial concentration of Nb(V).

Second-order rate expressions were also tested, but the first-order expressions (Eq. 5 and 6) gave much better fits to the data.

Figure 6 also shows that the limiting currents for reduction of Nb(V) and oxidation of Nb(IV) are almost the same at similar concentrations, indicating that the diffusion coefficient of the Nb(IV)-fluoride is about the same as that of NbF_7^{2-}.

Oxide oxidation measurements at glassy carbon electrodes.— Polyakova *et al.*[3] have shown that a glassy carbon electrode can be used to detect tantalum-oxofluoride complexes quantitatively in FLINAK melts. Haarberg *et al.*[30] used the same method to determine the amount of CaO dissolved in a $CaCl_2$ melt. The oxides in the oxocomplexes are oxidized at positive potentials, and the peak currents of sweep voltammograms can be used to measure the concentration of oxide species in the melt. Our experiments show that this is also possible for niobium-oxofluoro complexes. Figure 7 shows staircase voltammograms recorded at a glassy carbon electrode. Staircase voltammetry was found to give slightly more reproducible measurements than regular linear-sweep voltammetry or square-wave voltammetry. The melt was FLINAK with 1 mol % K_2NbF_7 and excess Nb metal to which Na_2O was added gradually. The figure shows that the voltammograms are rather noisy, making it difficult to determine precisely the peak currents. Therefore, instead of using the peak current as a measure, the area below the voltammograms has been used. Since the potential axis also is a time axis, this area is the time integral of the current and, consequently, a measure of the charge transferred through the cell during recording of the voltammogram. The areas below voltammograms as a function of the amount of oxide added to three different melts are given in Fig. 8. The three melts contained FLINAK with 1 mol % K_2NbF_7 and excess Nb metal, 0.5 mol % Nb_2O_5, and 0.3 mol % $KNbO_3$ before oxide additions. The plot in Fig. 8 is discussed later.

The molar ratio between oxide and niobium is expressed in the following as n_O°/n_{Nb}°. The amount of Na_2O added is used as the basis for n_O°, while the sum of the niobium added as K_2NbF_7 and the amount of Nb metal dissolved according to Eq. 4 before addition of oxide defines the value of n_{Nb}°.

Figure 5. LSV of a FLINAK melt to which 1 mol % K_2NbF_7 was added. The voltammogram was recorded 23.75 h after addition of K_2NbF_7. Temperature 700°C. Sweep rate 0.005 V s^{-1}. Pt reference, working, and counter electrodes. Area of working electrode 0.044 cm^2.


Figure 6. Anodic and cathodic limiting currents of a FLINAK melt to which 1 mol % K_2NbF_7 was added. The limiting currents were measured as functions of the time after addition of K_2NbF_7. Figure 5 shows an example of the limiting currents in this figure. (○) Cathodic limiting currents, (■) anodic limiting currents and (—) fitted curves based on a first-order reaction rate.
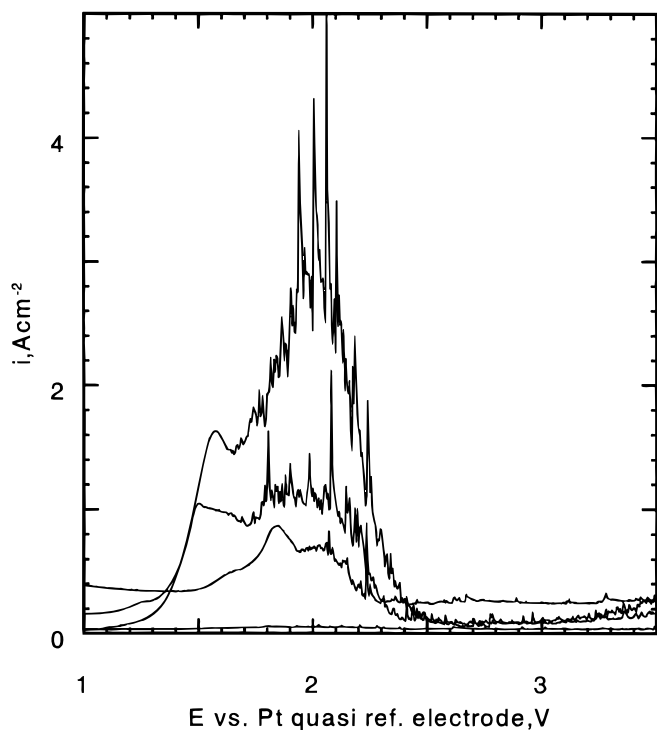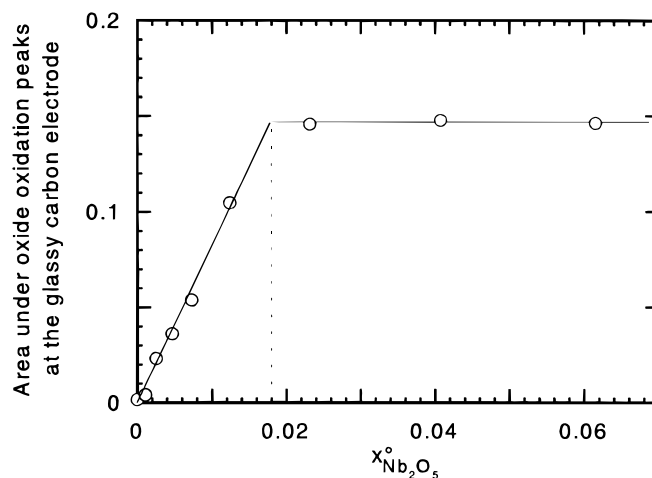
Figure 7. Four staircase voltammograms of a FLINAK melt containing 1 mol % K_2NbF_7, excess Nb metal, and varying amounts of Na_2O recorded at a glassy carbon electrode. The amount of Na_2O added (from the bottom curve and up): 0, 0.37, 1.06, and 1.65 mol %. Temperature 700°C. Parameters for the staircase voltammograms: step length 5 mV, step time 5 ms. Area of glassy carbon electrode: 0.051 cm².

Solubility of KNbO_3 and Nb_2O_5 in FLINAK at 700°C.—The solubilities of Nb_2O_5 and $KNbO_3$ were measured by adding the salts stepwise to FLINAK melts and after equilibration to record oxide oxidation voltammograms at a glassy carbon electrode. The solubility limit is reached when additional salt does not lead to increasing currents for the voltammograms. Figures 9 and 10 give the area below the
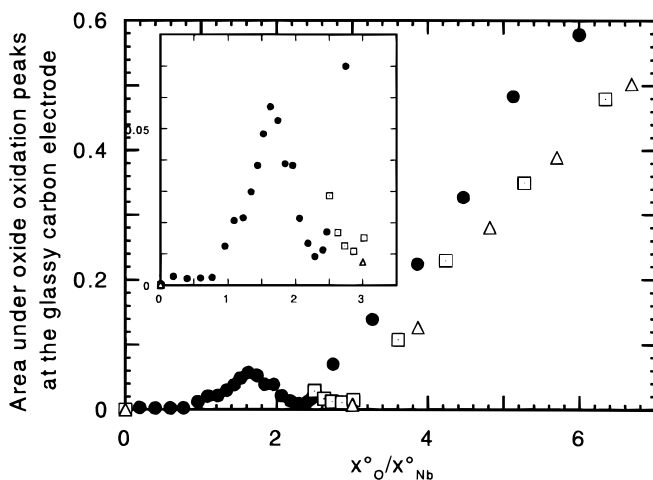
Figure 8. The area below voltammograms such as those in Fig. 7 plotted *vs.* the oxide to niobium ratio, n_O°/n_{Nb}°, in three different melts. The inset figure shows the n_O°/n_{Nb}° range up to 3.5 in more detail. The melts were (●) FLINAK containing 1 mol % K_2NbF_7, excess Nb metal and varying amounts of Na_2O, (⊡) FLINAK containing 0.5 mol % Nb_2O_5 and varying amounts of Na_2O, (△) FLINAK containing 0.3 mol % $KNbO_3$ and varying amounts of Na_2O. The areas for the latter melt have been divided by 0.3 to correct for the lower niobium content compared to the two other melts. Temperature for all melts: 700°C. Area of glassy carbon electrode: 0.051 cm².
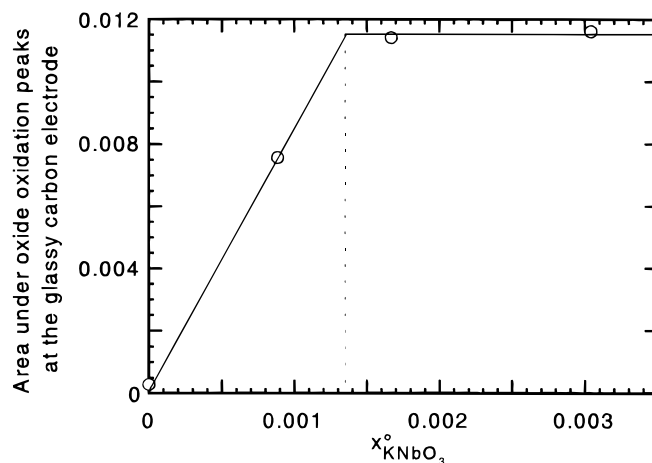

Figure 9. The solubility of Nb_2O_5 in FLINAK at 700°C. Staircase voltammograms were recorded at a glassy carbon electrode, and the areas below the oxide oxidation peaks obtained are plotted *vs.* n_O°/n_{Nb}° in the figure.

voltammograms as a function of the amount of salt added. They show that the nominal solubilities of Nb_2O_5 and $KNbO_3$ are 1.8 and 0.13 mol %, respectively. Matthiesen *et al.*,[17] using chemical analysis of melt samples extracted from a FLINAK melt at 700°C, found the same solubilities.

Nb(IV)-oxofluoride complexes in FLINAK.—Figure 11 shows a cyclic voltammogram of a FLINAK melt to which 1 mol % K_2NbF_7, excess Nb metal, and 0.9 mol % Na_2O were added. As previously reported,[2,4,22] no reduction peak except for the deposition peak is observed. There is, however, a reduction shoulder less than 100 mV positive of the reduction peak which is discussed in the following.

Linear-sweep voltammograms (LSVs) were recorded positively from the rest potential at a sweep rate of 5 mV s^{-1}. An example of such a voltammogram is given in Fig. 12. The FLINAK melt contained 1 mol % K_2NbF_7, excess Nb metal, and 0.46 mol % Na_2O. Two limiting-current levels are observed, one at *ca.* 0.4 V and the other at *ca.* 1.1 V. When no oxide is added to the melt, only the level at more positive potentials is present. This is the limiting current for the oxidation of Nb(IV)-fluoride complexes to NbF_7^{2-}. At oxide to niobium ratios above 0.8, however, only the level at more negative potentials is present in the voltammograms. A plot of the two limiting currents as functions of the oxide to niobium ratio is given in Fig. 13. The limiting current of the oxidation of Nb(IV)-fluoride


Figure 10. The solubility of $KNbO_3$ in FLINAK at 700°C. Staircase voltammograms were recorded at a glassy carbon electrode, and the areas below the oxide oxidation peaks obtained are plotted *vs.* n_O°/n_{Nb}° in the figure.
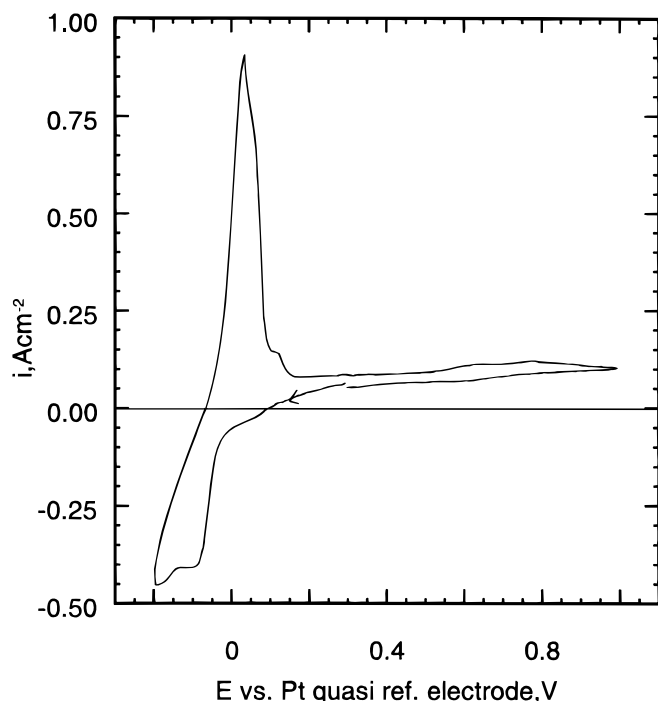
**Figure 11.** Cyclic voltammogram of a FLINAK melt containing 1 mol % K_2NbF_7, excess Nb metal, and 0.9 mol % Na_2O at 700°C. Sweep rate 0.2 V s^{-1}. Pt reference, working, and counter electrodes. Area of working electrode 0.044 cm^2.

complexes to NbF_7^{2-} is the difference between the total current at anodic potentials (*ca.* 1 V) and the limiting current for the oxidation at more negative potentials (*ca.* 0.3 V). The figure shows that the limiting current for the oxidation of Nb(IV)-fluorides to NbF_7^{2-} drops to zero at $n_O^\circ/n_{Nb}^\circ \approx 0.8$. Thus, the concentration of Nb(IV)-fluoro complexes reaches zero at this oxide to niobium ratio. At the same ratio, the limiting current for the oxidation taking place at more negative potentials reaches its maximum. It is therefore reasonable to assume that the Nb(IV)-fluoro complexes in the melt react with the added oxide to form Nb(IV)-oxofluoro complexes according to the reaction

$$NbF_x^{(x-4)-} + aO^{2-} \rightleftharpoons NbO_aF_y^{(y+2a-4)-} + (x-y)F^- \quad [7]$$
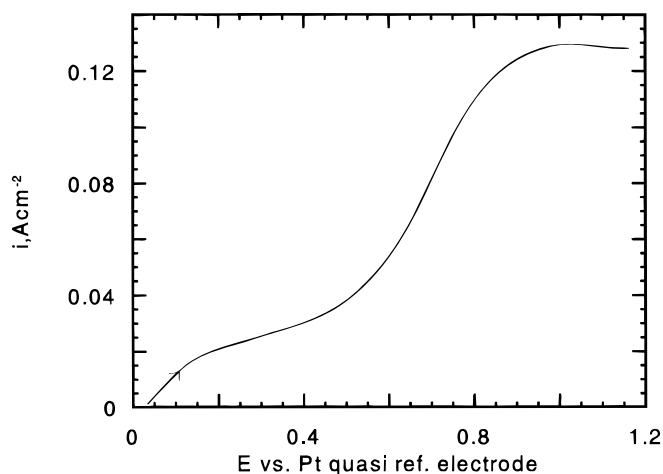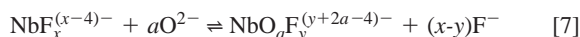
Figure 12. LSV recorded at 5 mV s^{-1} of a FLINAK melt containing 1 mol % K_2NbF_7, excess Nb metal, and 0.46 mol % Na_2O. Temperature 700°C. The figure shows two limiting-current levels, one at about 0.3 V and a second at about 1 V.
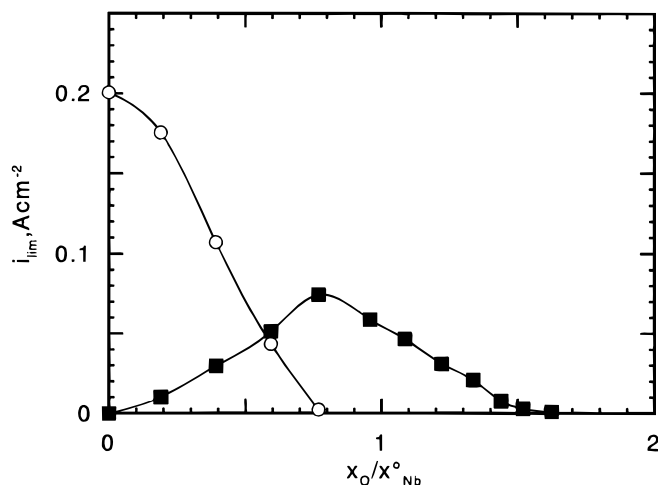
Figure 13. Limiting currents for the two limiting current levels observed in Fig. 12 as functions of n_O°/n_{Nb}° in the melt. The melt was FLINAK containing 1 mol % K_2NbF_7, excess Nb metal, and varying amounts of Na_2O. Temperature 700°C. (○) Limiting currents of the oxidation at about 1 V in Fig. 12 and (■) limiting currents of the oxidation at about 0.3 V in Fig. 12.

This implies that both the $NbOF_y^{(y-2)-}$ and $NbO_2F_y^{y-}$ complexes form in the melt, in agreement with the data of Matthiesen *et al.*[17] The reason the reduction/oxidation of the Nb(IV)oxofluoro complexes is observed only as a shoulder in the cyclic voltammogram in Fig. 11 is that the potential for the reduction

$$NbOF_5^{2-} + e^- \rightleftharpoons NbO_aF_y^{(y+2a-4)-} + (5-y)F^- + (1-a)O^{2-} \quad [8]$$
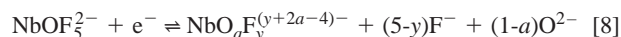
is close to the deposition potential. The shoulder in Fig. 11 is not present in melts without oxide. Due to the overlap of the reduction in Eq. 8 and the deposition reaction, characterization of the reduction with respect to reversibility, the number of electrons transferred, or diffusion coefficients has been impossible.

Figure 14 shows LSVs recorded at a Pt electrode. The melts were FLINAK with additions of K_2NbF_7 + Na_2O (n_O°/n_{Nb}° = 2), K_2NbF_7 + Nb metal + Na_2O (n_O°/n_{Nb}° = 1.6), and Nb_2O_5. The voltammograms are quite similar, indicating that the same species is being reduced in all three melts. There are two reduction steps, one at −0.4 V and a second at −0.85 V. The first step is a deposition step. Matthiesen *et al.*[4] performed potentiostatic electrolysis at the potential of the first reduction step, but the deposit did not adhere to the Pt electrode. Thus, identification of the material that deposits in the first reduction step is difficult. Voltammograms recorded shortly after each other gave reproducible peak currents for the first reduction step, while those of the second step changed considerably. It is therefore possible that the second step is not due to reduction of a species dissolved in the melt; it may as well be caused by further reduction of the material deposited in the first step.

Measurements of melts with $n_O^\circ/n_{Nb}^\circ \geq 3$. —Voltammograms of FLINAK melts to which 0.5 mol % Nb_2O_5 + Na_2O or 0.3 mol % $KNbO_3$ + Na_2O were added were alike at comparable n_O°/n_{Nb}° values. Similar voltammograms were also recorded of melts to which 1 mol % K_2NbF_7, excess Nb metal, and Na_2O were added, except that n_O°/n_{Nb}° was shifted to lower values.
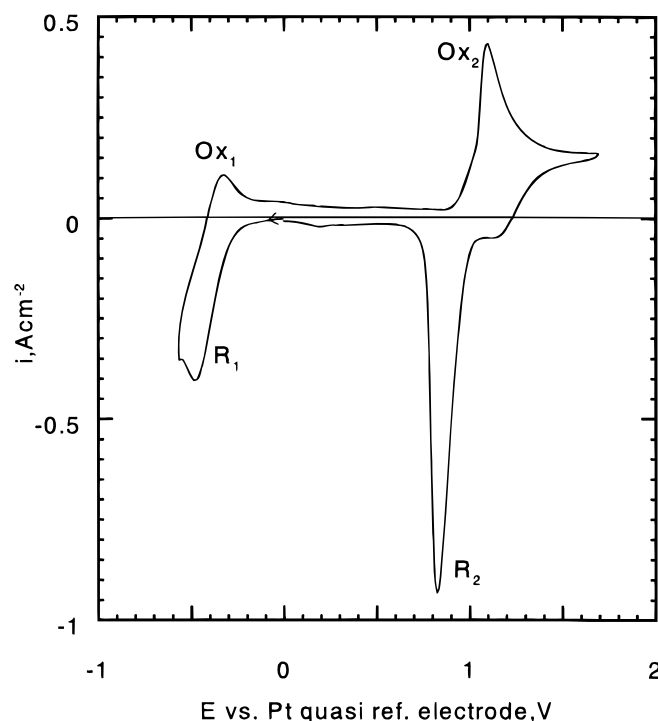
For n_O°/n_{Nb}° values between three and four (somewhat lower for the melt containing 1 mol % K_2NbF_7, excess Nb metal, and Na_2O), only minor changes were observed in the voltammograms recorded at the Pt electrode, the main change being a slight decrease of the measured currents. In this n_O°/n_{Nb}° range, cathodic currents were only slightly higher than the background current of the FLINAK melts. At the glassy carbon electrode, however, currents of the oxide oxidation peaks increased linearly with the amount of Na_2O added, as observed in Fig. 8. This indicates that the dissolved oxide species cannot be reduced within the electrochemical window of the FLINAK melt. When the oxide to niobium ratio, n_O°/n_{Nb}°, increased above 4, the typical
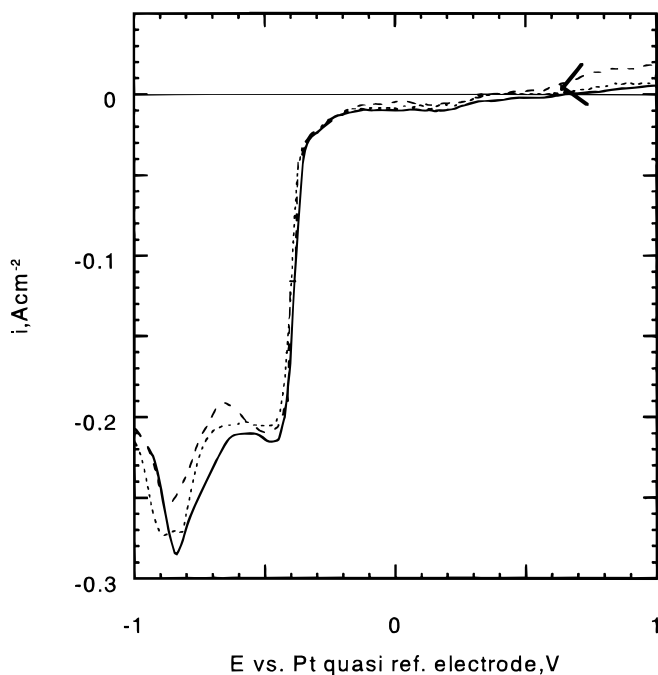
Figure 14. LSVs of FLINAK melts with additions of (——) 1 mol % K_2NbF_7 and 2 mol % Na_2O ($n_O^\circ/n_{Nb}^\circ = 2$), (- - -) 1 mol % Nb_2O_5, (— — —) 1 mol % K_2NbF_7, excess Nb metal, and 2 mol % Na_2O ($n_O^\circ/n_{Nb}^\circ = 1.6$). Pt working, reference, and counter electrodes, area of working electrode 0.044 cm². Temperature 700°C. Sweep rate 0.5 V s⁻¹.

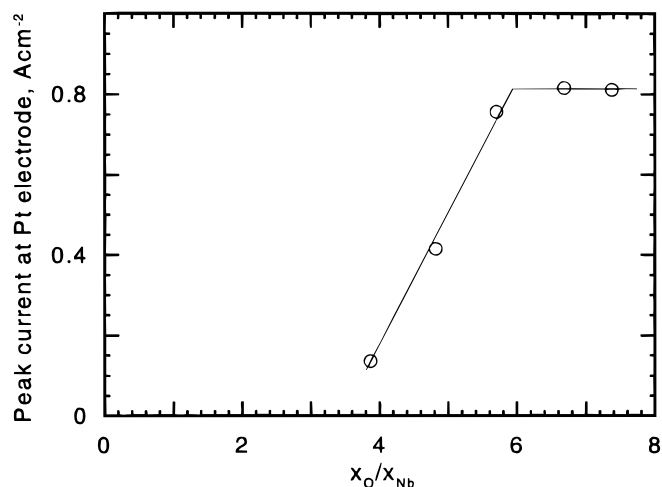deposition/dissolution peaks recorded at the Pt electrode disappeared and new peaks appeared. Figure 15 shows such a voltammogram.

Voltammograms in the oxide-rich region are characterized by a reduction/oxidation, R_1/Ox_1, (Figure 15) slightly positive of the alkali metal deposition peak and an oxidation/reduction, Ox_2/R_2, about 1.5 V above the reduction step. The current of both redox couples increased with increasing amounts of Na_2O added. The origins of these peaks were studied in a separate experiment. Na_2O was added to a FLINAK melt without niobium to study the electrochemical behavior of the noncomplexed O^{2-} ion. Voltammograms of these melts showed the redox couple Ox_2/R_2, but not the more negative couple R_1/Ox_1. The current for the oxidation peak Ox_2 increased linearly with the concentration of Na_2O. 0.22 mol % K_2NbF_7 was added to the melt, giving an n_O°/n_{Nb}° value of 5.6, and then the redox couple R_1/Ox_1 appeared. It is therefore reasonable to assume that the reduction/oxidation close to the alkali metal deposition, R_1/Ox_1, is due to niobium species, and that the oxidation/reduction Ox_2/R_2 is due to noncomplexed or weakly bonded O^{2-}. An oxidation reaction on platinum due to O^{2-} ions was also observed by Inman and Weaver[31] using a LiCl-KCl eutectic melt with additions of Li_2O. The shapes of the reduction peak R_1 and the corresponding oxidation peak Ox_1 indicate that the reduction/oxidation involves only soluble species, since the characteristic shapes of deposition/stripping peaks are absent. Moreover, the large value of the ratio between the current of the reduction peak and the corresponding current of the oxidation peak indicates that reduction R_1 is partly irreversible. This irreversibility decreased with increasing sweep rates, but was present even at sweep rates as high as 20 V s⁻¹. The peak current of the reduction step R_1 was measured using square wave voltammetry, and the peak currents are plotted *vs.* n_O°/n_{Nb}° in Fig. 16. The figure shows that the peak currents increase linearly with the amount of Na_2O added until $n_O^\circ/n_{Nb}^\circ \approx$ 6. Further additions of oxide did not cause increasing peak currents. The leveling out of the peak current at n_O°/n_{Nb}° values close to six was also found when Na_2O was added to melts containing Nb_2O_5 or K_2NbF_7 and Nb metal. The presence of dissolved niobium species in FLINAK melts with $n_O^\circ/n_{Nb}^\circ \geq 3$ is discussed later.

Equilibrium, sampling, and analysis of O^{2-} and Nb(V) in FLINAK with varying n_O^o/n_{Nb}^o ratios.—The influence of Na_2O on K_2NbF_7 containing FLINAK melts was studied as a function of n_O°/n_{Nb}° molar ratios at 700°C. The oxide and niobium contents in both the melt and in the solid phases are included in this ratio, which is therefore equal to the total amount of both Na_2O and K_2NbF_7 added. The oxide and Nb(V) concentrations in the melt are plotted *vs.* the n_O°/n_{Nb}° ratio in Fig. 17. From the following observations, it is possible to give an evaluation of the stoichiometry of the precipitating species as well as an idea of the complexes formed.

Figure 15. Cyclic voltammogram of a FLINAK melt containing 0.30 mol % $KNbO_3$ and 1.6 mol % Na_2O, $n_O^\circ/n_{Nb}^\circ = 7.4$. Platinum working electrode, area 0.044 cm². Sweep rate: 0.5 V s⁻¹. Temperature 700°C.


Figure 16. Peak currents of square-wave voltammograms recorded at a platinum electrode (area 0.044 cm²) plotted *vs.* n_O°/n_{Nb}°. The reduction studied is R_1 in Fig. 15. The melt was FLINAK containing 0.3 mol % $KNbO_3$ and varying amounts of Na_2O. Temperature 700°C. Parameters for the square-wave voltammograms: step length 5 mV, amplitude 20 mV, frequency 200 Hz.

$n_O^o/n_{Nb}^o = 0$.—The pure fluoride melt was stable at least up to 25 h at 700°C. Samples of this melt were always white, in contrast to melts containing Nb(IV).[17]

$0 < n_O^o/n_{Nb}^o < 2$.—The niobium concentration in the melt was constant, and the oxygen concentration increased linearly as n_O^o/n_{Nb}^o increased, indicating that all added oxide went into solution. The solubility results are therefore consistent with the formation of $NbOF_5^{2-}$ and $NbO_2F_4^{3-}$ complexes in the melt, as suggested by von Barner *et al.*[1] ($y = 1$ or 2)

$$y\, O^{2-} + NbF_7^{2-} \rightleftharpoons NbO_yF_x^{(2y+x-5)-} + (x\text{-}7)F^- \qquad [9]$$
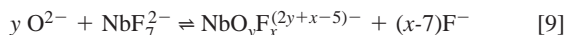
$2 < nO/n_{Nb} < 3$.—As shown in Fig. 17, the concentrations of both oxygen and niobium decrease as the ratio n_O^o/n_{Nb}^o increases and reach a solubility minimum at $n_O^o/n_{Nb}^o = 3$. Precipitation of a solid compound, probably AlkNbO$_3$, as indicated by Eq. 10, seems to occur, in agreement with Matthiesen *et al.*[17] and the voltammetric studies

$$NbO_2F_4^{3-} + O^{2-} + Alk^+ \rightleftharpoons AlkNbO_3(s) + 4F^- \qquad [10]$$
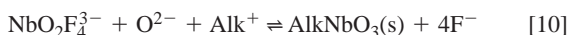
In this case, the relative slopes of the lines showing the decreasing Nb(V) and O^{2-} concentrations in the melt should be close to -1 and -2, respectively. The data presented in Fig. 17 show slightly less negative slopes, and this is discussed elsewhere.[18] The measured solubility seems to be caused by the presence of a species like $NbO_3F_3^{3-}$.[18]

$3 < n_O^o/n_{Nb}^o < 4.6$.—Dissolution of AlkNbO$_3$(s) occurs. The concentrations of both oxygen and niobium increases up to the ratio $n_O^o/n_{Nb}^o = 4$. The experimental data indicated that all solids are dissolved at this point. Matthiesen *et al.*[17] proposed the formation of $NbO_yF_x^{(2y+x-5)-}$ complexes, probably with $y = 4$. When the ratio n_O^o/n_{Nb}^o exceeds 4, the niobium concentration remains constant while the oxygen composition in the melt increases. The increase, however, is less than what would be expected if all the added oxide dissolves completely, indicating the possible formation of another solid compound.

Based on the present data only, it is not possible to give a final conclusion on the Nb(V)-O-F complexes formed in the concentration region $0 < n_O^o/n_{Nb}^o < 4.6$. Recently, Vik *et al.*[18] showed by Raman spectroscopy that a melt consisting of K$_2$NbF$_7$ in FLINAK with varying Na$_2$O concentrations up to $n_O^o/n_{Nb}^o = 8$ probably contained several Nb(V)-O-F complexes with various stoichiometry depending on the O/Nb molar ratio.
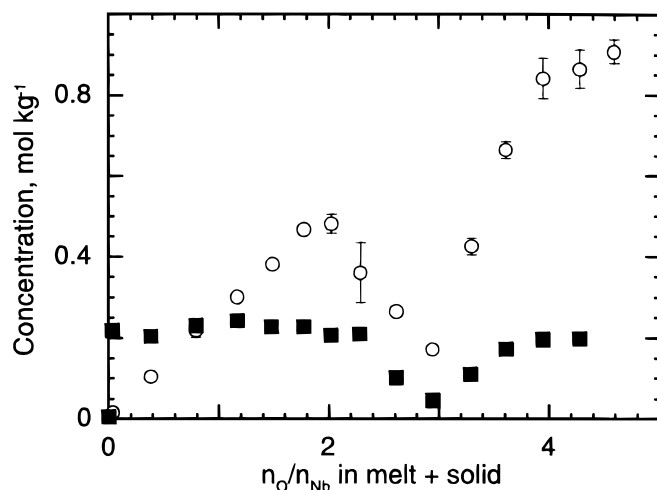

Figure 17. Na$_2$O and Nb(V) concentrations in the liquid LiF-NaF-KF eutectic at 700°C *vs.* the molar ratio of the total amount of oxide and niobium in the melt and in the solid phases, n_O^o/n_{Nb}^o. (○) Oxide analysis with standard deviation and (■) Nb analysis, standard deviations less than size of squares.

Discussion

Spontaneous reduction of Nb(V)-fluorides.—The reduction of Nb(V)-fluorides has also been observed by Alimova *et al.*,[32] and by Stöhr.[10] Stöhr also observed spontaneous reduction of Nb(V) in FLINAK but found that longer times were required for complete conversion of Nb(V) to Nb(IV) than observed in our electrochemical study. Alimova *et al.*[32] found that Nb(V) was reduced to Nb(IV) when K$_2$NbF$_7$ was added to an alkali chloride melt. It is, however, rather surprising that Nb(V)-fluorides are reduced spontaneously in FLINAK. Reduction of Nb(V) to Nb(IV) requires oxidation of other species. Positively scanned voltammograms of melts containing Nb(V)-fluorides show no oxidation other than oxidation of the platinum working electrode close to 1 V above the reduction of Nb(V) to Nb(IV). Similar scans at a glassy carbon electrode show only oxidation of the very small amount of oxide impurities in the melt taking place about 1.5 V positive of the reduction of Nb(V) to Nb(IV). Moreover, neither the platinum electrodes nor the glassy carbon crucible showed any signs of corrosion after finishing the experiments. It is therefore unlikely that platinum or glassy carbon is oxidized during reduction of Nb(V)-fluorides. Reduction of Nb(V) to Nb(IV) has also been observed in alkali chloride melts.[13] However, in such melts, the reduction of Nb(V) to Nb(IV) takes place at potentials only slightly below the oxidation of chloride to chlorine, and the reaction

$$Nb(V) + Cl^- \rightleftharpoons Nb(IV) + \frac{1}{2}Cl_2(g) \qquad [11]$$
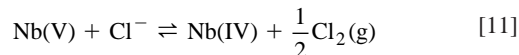
is expected to take place. Chlorine evolution has been observed when Nb(V) chlorides have been added to alkali chloride melts.[33] A similar reaction in FLINAK melts involving oxidation of fluoride to fluorine is not expected. The oxidation potential of fluorides compared to fluorine is considerably higher than the oxidation of chloride to chlorine, and the reduction of Nb(V)-fluorides compared to Nb(V) chlorides is much more negative. Consequently, one should expect that ΔG for the reaction

$$Nb(V) + F^- \rightleftharpoons Nb(IV) + \frac{1}{2}F_2(g) \qquad [12]$$
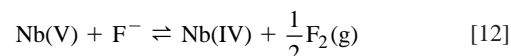
is too positive for the reaction to occur. Nevertheless, Alimova *et al.*[32] report that fluoride is oxidized when K$_2$NbF$_7$ is added to an alkali chloride melt. Analysis of the melt after spontaneous reduction of Nb(V) to Nb(IV) showed that the amount of fluoride ions in the melt had decreased. They also present other quite convincing results indicating that Eq. 12 occurred. One should also bear in mind that Eq. 12 is thermodynamically possible if the fluorine pressure is sufficiently low, which is the case if the fluorine that escapes the melt reacts with, *e.g.,* the iron materials in the cold zones inside the furnace. Equation 12 is also in agreement with the first-order reaction mechanism observed in the present work.

It should be noted that these results disagree with the observations made during the present solubility experiments. After K$_2$NbF$_7$ had been added to the melt, it was left to equilibrate for about 24 h before the first sample was withdrawn and Na$_2$O was added. According to Fig. 6, about 50% of the Nb(V)F$_7^{2-}$ originally present should be reduced to Nb(IV)F$_x^{(x-4)-}$. From similar solubility experiments with Nb(IV),[17] it is known that samples of melts with Nb(IV)fluoride complexes have a distinct blue color, but this color was never observed in any of the samples withdrawn from the melt in the present solubility experiment. The reaction mechanism of Reaction 12 seems to vary from one investigation to another. One speculates that the rate may, *e.g.,* depend on the ability of the materials used in the cell to react with fluorine escaping from the melt, or on the catalytic effect of small impurities in the melt.

The spontaneous reduction of Nb(V) to Nb(IV) does not occur for the NbOF$_5^{2-}$ complex. An explanation for this can be found by considering the voltammogram in Fig. 12. The figure shows that the reduction of NbF$_7^{2-}$ takes place about 0.8 V above the reduction of NbOF$_5^{2-}$ to the Nb(IV)-oxofluorocomplex. The reaction

$$Nb(V)F_7^{2-} + Nb(IV)OF_x^{(x-2)-} \rightleftharpoons Nb(V)OF_5^{2-}$$

$$+ Nb(IV)F_y^{(y-4)-} + (y-x)F^- \quad [13]$$
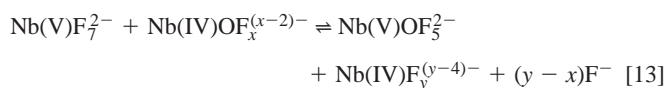
will therefore be strongly shifted to the right ($\Delta G = -nF\Delta E \approx -77$ kJ). This indicates that oxide stabilizes niobium in the oxidation state five.

Oxide oxidation measurements at the glassy carbon electrode.—A further discussion of the data in Fig. 8 is required. Polyakov *et al.*[3] measured the oxide oxidation peak currents of LSVs at a glassy carbon electrode. When they added Na_2O to a FLINAK melt containing K_2TaF_7, they found that the peak currents increased linearly with the amount of Na_2O added until $n_O^o/n_{Ta}^o = 2$, then decreased linearly until $n_O^o/n_{Ta}^o = 3$, and then increased again when Na_2O was added beyond $n_O^o/n_{Ta}^o = 3$. The increasing currents measured for $n_O^o/n_{Ta}^o \geq 3$ were explained simply by assuming that the added Na_2O dissolved and dissociated in the melt. The O^{2-} ions were oxidized at the glassy carbon electrode, resulting in higher currents. This, however, is not correct, as shown by Vik *et al.*[34] When Na_2O is added beyond $n_O^o/n_{Ta}^o = 3$, $KTaO_3$, which precipitated when $2 < n_O^o/n_{Ta}^o < 3$, dissolved in the same way as for the present system (Fig. 17). The plot in Fig. 8 apparently shows a somewhat different behavior. The amount of oxide in the melt, supposedly represented by the area below voltammograms such as those in Fig. 7, does not seem to increase with the first additions of Na_2O to the melt. There is a plateau for n_O^o/n_{Nb}^o values between 0 and 0.8, then there is a linear increase between 0.8 and 1.6, a decrease between 1.6 and 2.4, and finally a steady increase for higher n_O^o/n_{Nb}^o values. The experiment was made three times, and the same results were obtained each time.

Both the plateau and the nonintegral values at the transitions in Fig. 8 require further discussion. Starting with the plateau, Fig. 18 shows chronoamperograms recorded at various potentials at the glassy carbon electrode. A normal diffusion-controlled oxidation would give increasing currents with increasing overpotentials until the limiting-current level is reached. The chronoamperograms in Fig. 18 deviate from this behavior in that they show increasing currents until a certain overpotential, but increasing the potential above that value leads to decreasing currents. This is illustrated more clearly in Fig. 19 where the current measured 0.1 and 15 s after applying the potential is plotted *vs.* the potential applied. The shapes of the curves resemble the staircase voltammograms in Fig. 7, there being an increase of the current to a certain potential value, and then a sudden decrease. Such behavior indicates that the electrode passivates,
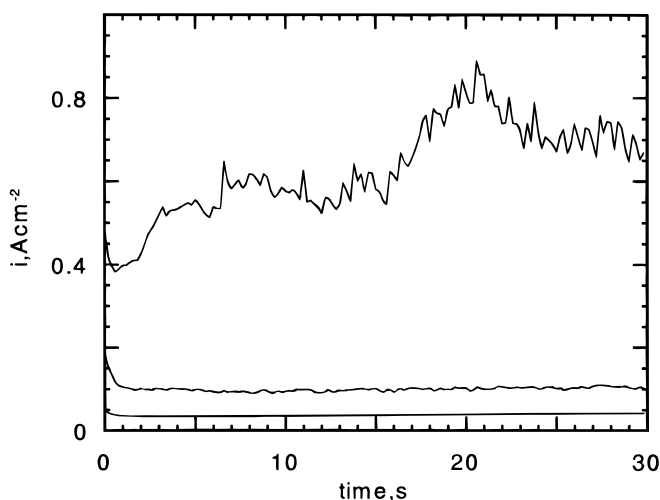
i.e., that the oxidation of oxide is hindered above a certain potential value. Passivation of graphite electrodes was also observed by Reddy *et al.*,[35] who studied the oxidation of oxide at a graphite anode in a Li_2O-LiF-CaF_2 melt at 1093 K. They report that the passivation is due to adsorption of CO on the electrode surface.

The plateau for $0 < n_O^o/n_{Nb}^o < 0.8$ in Fig. 8 can therefore be caused by a passivation of the glassy carbon electrode above a certain potential. Assuming that the oxide in Nb(IV)-monoxo-fluoro complex is so strongly bonded that the oxidation takes place mainly at potentials in the passive region of the glassy carbon electrode, only a minor part of the total oxide would be detected. However, oxide bonded to a Nb-dioxo-fluoro complex would probably be more weakly bonded and would consequently be oxidized at sufficiently negative potentials to be in the nonpassive potential region of the electrode. This would lead to considerably higher currents during the oxidation of the dioxo complex. The formation of a Nb-dioxo-fluoro complex can therefore explain the sharp increase at $n_O^o/n_{Nb}^o = 0.8$ in Fig. 8. A transition at $n_O^o/n_{Nb}^o = 0.8$ is also seen in Fig. 13, where the oxidation current of the Nb(IV)-fluoro to Nb(V)-fluoro complex reaches zero and the oxidation current of the Nb(IV)-monoxo-fluoro to the Nb(V)-monoxo-fluoro complex is at its maximum. The falling oxidation currents of the Nb(IV)-monoxo-fluoro complex above $n_O^o/n_{Nb}^o = 0.8$, together with the increase in the oxide oxidation currents seen in Fig. 8, indicate the formation of a new species. This species is probably a Nb-dioxo-fluoro complex.

A straightforward explanation for the n_O^o/n_{Nb}^o value at this transition has not been found. Efforts were made to study melts with $n_O^o/n_{Nb}^o = 0.8$ in the presence of excess Nb metal by Raman and infrared (IR) spectroscopy of the melt, but the experiments were unsuccessful. The melt was too strongly colored to allow recording of Raman spectra. To record IR spectra, a cell with a diamond window was to be used, but preliminary tests showed that a thin, shiny black layer, possibly niobium carbide, formed on diamond when it was in contact with the melt, making it unsuitable for IR spectroscopy.

The nonintegral values of the transitions at $n_O^o/n_{Nb}^o = 1.6$ and 2.4 also need discussion. Figure 14 shows that voltammograms of melts containing $n_O^o/n_{Nb}^o(V) = 2$ and $n_O^o/n_{Nb}^o(IV) = 1.6$ were similar. Moreover, only very low anodic currents were measured at potentials above the deposition peak, indicating that Nb in the dissolved Nb species was present in its most oxidized form, *i.e.,* as Nb(V). Stöhr[10] also found, when studying a FLINAK melt with excess Nb metal, that the anodic limiting current of the Nb(IV)-monoxo-fluoro complex reached zero at $n_O^o/n_{Nb}^o = 1.6$. Consequently, at $n_O^o/n_{Nb}^o = 1.6$, even in the presence of Nb metal, it is reasonable to assume that Nb(V)-dioxo-fluoro complexes, probably $NbO_2F_4^{3-}$, are the predominant dissolved Nb species. The following reaction is therefore
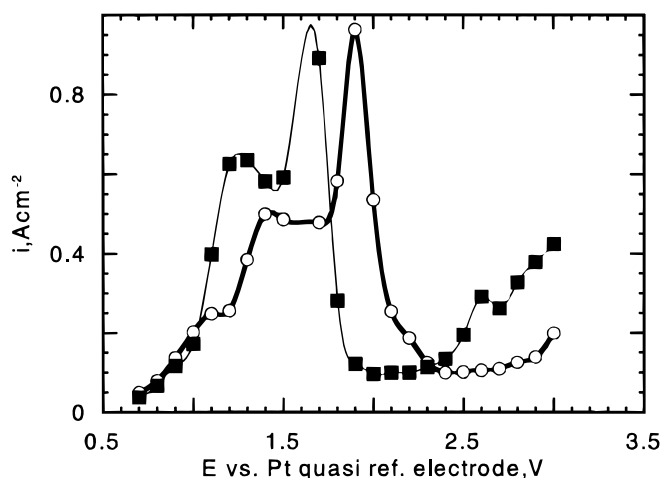

Figure 18. Chronoamperograms recorded at a glassy carbon electrode at three different potentials. The potentials were (bottom and up): 0.7, 2.3, and 1.5 V *vs.* a platinum quasi reference electrode. The FLINAK melt contained 1 mol % K_2NbF_7, excess Nb metal, and 2.3 mol % Na_2O. Temperature 700°C. Area of glassy carbon electrode 0.051 cm^2.

Figure 19. Samples of chronoamperograms such as those in Fig. 17 plotted *vs.* the applied potential. The times after application of the potentials from the rest potential are: (○) 0.1 s and (■) 15 s.

suggested to take place when oxide is added to a melt with Nb(IV)-monoxo-fluoro complexes

$$5Nb(IV)\text{-monoxo-fluoride} + O^{2-} \rightleftharpoons 4NbO_2F_4^{3-} + Nb(s) \quad [14]$$
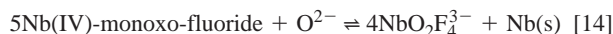
Due to the precipitation of Nb metal according to Eq. 14, the concentration of dissolved niobium in the melt decreases. When Eq. 14 is completely shifted to the right, the concentration of dissolved niobium species, n_{Nb}, is less than n_{Nb}° by a factor of 4/5. Thus, $n_O^\circ/n_{Nb} = 5/4 n_O^\circ/n_{Nb}^\circ$. Multiplying the n_O°/n_{Nb}° values 1.6 and 2.4 by 5/4, 2 and 3 are obtained, respectively. Figure 20 shows the same data as in Fig. 8 plotted *vs.* n_O°/n_{Nb}, *i.e.*, the molar fraction between oxide and niobium in the melt corrected for precipitation of Nb according to Eq. 14. Since no metal precipitation occurs in melts where Nb_2O_5 or $KNbO_3$ was used as the niobium source [only Nb(V) added], $n_{Nb} = n_{Nb}^\circ$ in these melts. The corrected plot shows a maximum at $n_O^\circ/n_{Nb} = 2$ and a minimum at 3. It also shows that the areas below the oxide oxidation voltammograms of melts with Nb_2O_5 and $KNbO_3$ compare well with those obtained from melts with excess Nb metal, supporting the assumption that Nb complexes with more than one oxide per niobium are stable only when Nb is in oxidation state five.

Matthiesen *et al.*[17] also reported a decrease in the niobium concentration when Na_2O was added to a Nb(IV) containing FLINAK melt at $n_O^\circ/n_{Nb}^\circ > 1$. However, they also observed that some of the oxide added above $n_O^\circ/n_{Nb}^\circ > 1$ did not go into solution. Two independent series of experiments were performed, and the slopes of the lines describing the changes in the Nb(IV) and O^{2-} compositions with additions of Na_2O indicate precipitation of a niobium oxide compound above $n_O^\circ/n_{Nb}^\circ = 1$. These solubility results are in contrast with the present voltammetric data, Fig. 8 and 20. The voltammetric data indicate that all oxide added until $n_O^\circ/n_{Nb}^\circ = 1.6$ is dissolved, while the melt analysis[17] showed that some oxide precipitated. A reasonable explanation for the apparent discrepancy in the two sets of data has not been found.

Niobium-oxo complexes in FLINAK melts with $n_O^\circ/n_{Nb}^\circ \geq 3$.—Polyakov *et al.*[3] assumed that noncomplexed O^{2-} ions caused the increasing currents measured during oxide oxidation for $n_O^\circ/n_{Ta}^\circ \geq 3$. In view of the present results, those of Matthiesen *et al.*[17] and Vik *et al.*,[34] this is not the case, neither for the niobium system nor the tantalum system. Using the peak current of the Ox_2 oxidation shown in Fig. 15, it is possible to detect O^{2-} concentrations at least as low as 0.05 mol %. Traces of noncomplexed O^{2-} ions were not detected below $n_O^\circ/n_{Nb} \approx 4$ (using the corrected n_{Nb}). Figure 20 shows, however, that the oxide oxidation currents increase from $n_O^\circ/n_{Nb} = 3$. Since noncomplexed oxide is not present in the range 3
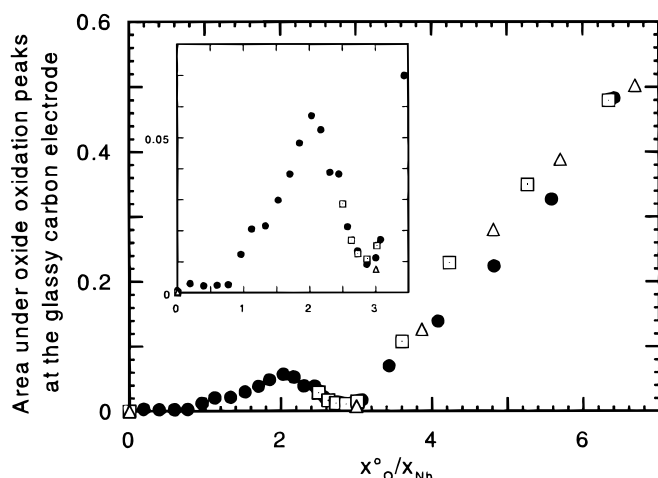
$< n_O^\circ/n_{Nb} < 4$, it is reasonable to assume that the rise in the oxide oxidation currents is due to niobium-oxo complexes. This means that solid $KNbO_3$ dissolves when Na_2O is added to the melt. However, for $3 < n_O^\circ/n_{Nb} < 3.8$, voltammograms recorded at the platinum electrode do not show any reductions of significance between the alkali metal reduction and the platinum oxidation. The soluble product of the reaction between $AlkNbO_3(s)$ and Na_2O in FLINAK therefore seems to be a niobium-oxo complex that is electroinactive except for the oxide oxidation at glassy carbon. At $n_O^\circ/n_{Nb} > 3.8$, a reduction step due to niobium species, R_1 in Fig. 15, appears.

We have not been able to give clear-cut explanations for all the reported observation, but some suggestions are given. Andonov *et al.*[21] have studied molten $LiNbO_3$ by neutron scattering. They found that niobium oxide clusters with niobium octahedrally coordinated by oxygen were present in the melt. These octahedra typically shared corners, forming quite ordered clusters. Moreover, Raman spectroscopic measurements of FLINAK melts containing 2.7 mol % K_2NbF_7 and relatively much Na_2O showed Raman bands which were assigned to NbO_6 octahedrals sharing corners or edges.[1] It is therefore possible that clusters similar to those observed by Andonov *et al.*[21] also exist in FLINAK melts. At $n_O^\circ/n_{Nb} > 3.8$, R_1 in Fig. 15 starts to appear, and at slightly higher n_O°/n_{Nb} values, oxidation of weakly bonded and noncomplexed O^{2-} ions (Ox_2 in Fig. 15) becomes significant. This indicates that new Nb species form as n_O°/n_{Nb} increase above 3.8, in agreement with Raman spectroscopic measurements[18] that indicate the presence of two Nb species at $n_O^\circ/n_{Nb} > 4$. These new species show both oxide oxidation at the glassy carbon electrode and reduction at the Pt electrode. Moreover, they exist in equilibrium with relatively large concentrations of noncomplexing O^{2-} ions. Figure 16 shows that the peak current for R_1 stops to increase at n_O°/n_{Nb} values close to six, indicating that Nb-oxo complexes with an oxide to niobium ratio, n_O/n_{Nb}, equal to six is stable in the melt. Thus, it is possible that the species first formed when Na_2O is added to a melt with $KNbO_3$ react with subsequently added oxide to form niobium-oxo complexes with $n_O/n_{Nb} = 6$. The reduction at R_1 in Fig. 15 may thus be due to such complexes. Since R_1 does not show completely reversible behavior, simple voltammetric analysis of this peak does not give precise results. However, the reversibility condition[29]

$$E_p - E_{p/2} = \frac{RT}{nF} \quad [15]$$

can give a rough estimate of the number of electrons transferred at R_1. Using relatively high sweep rates (1-10 V s^{-1}), n values around 0.8 were obtained. Possibly one Nb(V) ion is reduced to Nb(IV) for each species reduced, indicating that the Nb-oxo complex with $n_O/n_{Nb} = 6$ is monomeric.

Conclusion

The equilibria suggested to be valid for niobium complexes in a FLINAK melt containing excess Nb metal deduced from the electrochemical measurements are summarized as follows. With no oxide added to the melt only $Nb(IV)F_x^{(x-4)-}$ ions are present. When $n_O^\circ/n_{Nb}^\circ < 0.8$, $Nb(IV)F_x^{(x-4)-}$ and $Nb(IV)OF_y^{(y-2)-}$ coexist in the melt. At $0.8 < n_O^\circ/n_{Nb}^\circ < 2$, some inconsistency between the present voltammetric data and the solubility data of Matthiesen *et al.*[17] is apparent. The solubility data[17] indicate that $Nb(IV)OF_y^{(y-2)-}$, $Nb(IV)O_2F_y^{y-}$, and a solid niobium-oxo-compound are formed. The present voltammetric data, however, indicate that only Nb(V) is stable at these high oxide concentrations, and that an equilibrium of the type $5Nb(IV)\text{-monoxo-fluoride} + \text{oxide} \rightleftharpoons 4NbO_2F_4^{3-} + Nb(s)$ shifted heavily to the right is established. At $2 < n_O^\circ/n_{Nb}^\circ < 3$, $NbO_2F_4^{3-}$ reacts with O^{2-} and $KNbO_3(s)$ is formed. Nb_2O_5 dissolves according to the reaction $Nb_2O_5 + 4F^- + K^+ \rightleftharpoons NbO_2F_4^{3-} + KNbO_3(s)$, in agreement with the data of Matthiesen *et al.*[17] At higher oxide to niobium ratios, $KNbO_3(s)$ dissolves, and Nb(V)-O-F complexes with higher O/Nb ratios are formed. This is also shown by Raman spectroscopy.[18] The stability of Nb(V) in FLINAK in the absence of oxide seems to depend on the experimental setup. Some

Figure 20. The same data as those in Fig. 8 plotted *vs.* n_O°/n_{Nb}, is the ratio between the amount of oxide added and the amount of niobium in the melt corrected for the precipitation of Nb metal according to Eq. 14 (see text).

investigations show that Nb(V) is slowly and spontaneously reduced to Nb(IV), while others show no reduction. We have not been able to resolve this apparent discrepancy.

References

1. J. H. von Barner, E. Christensen, N. J. Bjerrum, and B. Gilbert, *Inorg. Chem.,* **30,** 561 (1991).
2. E. Christensen, X. Wang, J. H von Barner, T. Østvold, and N. J. Bjerrum, J. *Electrochem. Soc.,* **141,** 1212 (1994).
3. L. P. Polyakova, E. G. Polyakov, F. Matthiesen, E. Christensen, and N. J. Bjerrum, *J. Electrochem. Soc.,* **141,** 2982 (1994).
4. F. Matthiesen, E. Christensen, J. H. von Barner, and N. J. Bjerrum, *J. Electrochem. Soc.,* **144,** 1793 (1996).
5. P. Chamelot, B. Lafage, and P. Taxil, *Electrochim. Acta,* **43,** 607 (1997).
6. P. Chamelot, B. Lafage, and P. Taxil, *J. Electrochem.Soc.,* **143,** 1570 (1996).
7. B. Gillesberg, N. J. Bjerrum, and J. H. von Barner, *J. Electrochem. Soc.,* **144,** 3435 (1997).
8. V. Van, A. Silny, and V. Danek, *Electrochem. Commun.,* **1,** 354 (1999).
9. V. Van, A. Silny, J. Hives, and V. Danek, *Electrochem. Commun.,* **1,** 295 (1999).
10. U. Stöhr, Ph.D. Thesis, Fakultät für Chemie, Universität Karlsruhe (TH) (1997).
11. M. Bachtler, J. Rockemberger, W. Freyland, C. Rosenkilde, and T. Østvold, *J. Phys. Chem.,* **98,** 742 (1994).
12. C. Rosenkilde and T. Østvold, *Acta Chem. Scand.,* **48,** 732 (1994).
13. C. Rosenkilde and T. Østvold, *Acta Chem. Scand.,* **49,** 85 (1995).
14. C. Rosenkilde and T. Østvold, *Acta Chem. Scand.,* **49,** 265 (1995).
15. C. Rosenkilde, G. A. Voyiatzis, and T. Østvold, *Acta Chem. Scand.,* **49,** 405 (1995).
16. C. Rosenkilde, G. A. Voyiatzis, V. R. Jensen, M. Ystenes, and T. Østvold, *Inorg. Chem.,* **34,** 4360 (1995).
17. F. Matthiesen, P. Jensen, and T. Østvold, *Acta Chem. Scand.,* **52,** 1000 (1998).
18. Aa. Vik, V. Dracopoulos, G. N. Papatheodorou, and T. Østvold, *J. Alloys Compd.* To be published.
19. M. D. Fontana, G. E. Kugel, G. Metrat, and C. Carabatos, *Phys. Status Solidi B,* **103,** 211 (1981), and references therein.
20. A. A. McConnell, J. S. Anderson, and C. N. R. Rao, *Spectr. Acta,* **32A,** 1067 (1976).
21. P. Andonov, P. Chieux, and S. Kimura, *Phys. Scr.,* **T57,** 36 (1995).
22. V. I. Konstantinov, E. G. Polyakov, and P. T. Stangrit, *Electrochim. Acta,* **26,** 445 (1981).
23. J. H. von Barner, R. W. Berg, Y. Berghoute, and F. Lantelme, *Molten Salt Forum,* **12,** 121 (1993/94).
24. G. W Horsby, *J. Iron Steel Inst.,* 43 (1956).
25. Q. Zhiyu and P. Taxil, *J. Appl. Electrochem.,* **15,** 250 (1985).
26. M. Chemla and V. Grinevitch, *Bull. Soc. Chim. France,* 853 (1973).
27. A. Barhoun, F. Lantelme, M. E. de Roy, and J. P. Besse, *Mater. Sci. Forum,* **7375,** 313 (1991).
28. A. Khalidi, P. Taxil, P. Lafage, and A. P. Lamaze, *Mater. Sci. Forum,* **7375,** 421 (1991).
29. Southamptom Electrochemistry Group, *Instrumental Methods in Electrochemistry,* Ellis Horwood, West Sussex, England (1990).
30. G. M. Haarberg, N. Aalberg, K. S. Osen, and R. Tunold, in *Molten Salts,* C. L. Hussey, Y. Ito, G. Mamantov, D. A. Shores, and D. S. Newman, Editors, PV 94-13, p. 385, The Electrochemical Society Proceedings Series, Pennington, NJ (1994).
31. D. Inman, and M. J. Weaver, *J. Electroanal. Chem.,* **51,** 45 (1974).
32. Z. Alimova, E. Polyakov, L. Polyakova, and V. Kremenetskiy, *J. Fluorine Chem.,* **59,** 203 (1992).
33. L. Arurault, J. Bouteillon, J. de Lepinay, A. Khalidi, and J. C. Poignet, *Mater. Sci. Forum,* **73-75,** 305 (1994).
34. Aa. Vik, V. Dracopoulos, and T. Østvold, in *The International George Papatheodoro Symposium,* S. Boghosian, V. Dracopoulos, C. G. Kontoyannis, and G. A. Voyiatzis, Editors, Vol. 109, ICE, Forth, Patras, Greece (1999).
35. G. R Reddy, A. R. Narayan, and P. T. Velu, in *Ultra Large Scale Integration Science and Technology,* G. Celler, K. Hoh, and E. Middlesworth, Editors, PV 93-13, p. 385, The Electrochemical Society Proceeedings Series, Pennington, NJ (1994).